

## DIRECT LASER SINTERING OF BOROSILICATE GLASS

F. Klocke, A. McClung and C. Ader

Fraunhofer Institute for Production Technology IPT, Aachen, Germany

Reviewed, accepted August 4, 2004

### Abstract

Despite the advantages that selective laser sintering (SLS) offers in terms of material availability, many materials have yet to be explored for feasibility and even fewer are available on a commercial basis. This paper presents initial investigations for one such material, borosilicate glass, which could be of particular interest to filter manufacturers because it presents an attractive alternative to the conventional, time-consuming way of producing filters of various porosity classes. Process results are presented including a determination of the optimal parameter window and the effect of processing parameters on the density and surface quality. The effects of thermal post-processing and the inclusion of an additive are also discussed.

### Introduction

In order for new applications to emerge in solid freeform fabrication industry, materials need to be developed that match those used in conventional machining processes. However, the applicability of the material for the rapid process must be ensured. SLS in particular needs to be exploited for new material investigations, due to the fact that any material that can sinter or has a decaying viscosity curve can theoretically be employed. The borosilicate glass powder explored herein is one such material, which has potential interest to manufacturers of porous borosilicate glass products, such as filters and sensors.

Borosilicate glass can be classified as a standard glass. Thereby, by definition, it has the property that it exists in a vitreous state in which there is no long range atomic order. The glass powder employed herein is borosilicate glass type 3.3 with an average particle size of 30  $\mu\text{m}$  and a broad distribution range. The composition is largely  $\text{SiO}_2$  mixed with  $\text{B}_2\text{O}_3$ , **Fig. 1.** The presence of  $\text{B}_2\text{O}_3$  reduces the coefficient of thermal expansion, to about one-third that of standard soda-lime glass, and makes the glass more resistant to thermal shock [1]. As a glass, it has no exact melting point but rather is defined by its softening point, 820  $^\circ\text{C}$ , and by the glass transition temperature,  $T_g = 552$   $^\circ\text{C}$ . When heated above  $T_g$ , the glass properties of borosilicate transform into melt properties. The annealing point, where stress relaxation occurs, is 565  $^\circ\text{C}$  [2].

Element	% by weight
Silica ( $\text{SiO}_2$ )	80.60
Boron oxide ( $\text{B}_2\text{O}_3$ )	12.60
Sodium oxide ( $\text{Na}_2\text{O}$ )	4.20
Alumina ( $\text{Al}_2\text{O}_3$ )	2.20
Iron oxide ( $\text{Fe}_2\text{O}_3$ )	0.40
Calcium oxide ( $\text{CaO}$ )	0.10
Magnesium oxide ( $\text{MgO}$ )	0.05
Chlorine (Cl)	0.10

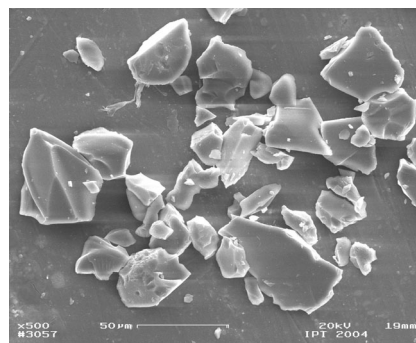


Fig. 1: Composition and SEM picture of borosilicate glass powder

## Experimental Results

In order to explore the feasibility of laser sintering of borosilicate glass, the process parameters for SLS, shown in **Figure 2**, need to be investigated in order to determine the optimal layer thickness  $d_n$ , laser power  $P_L$ , scan velocity  $v_s$  and hatch spacing  $h_s$ .

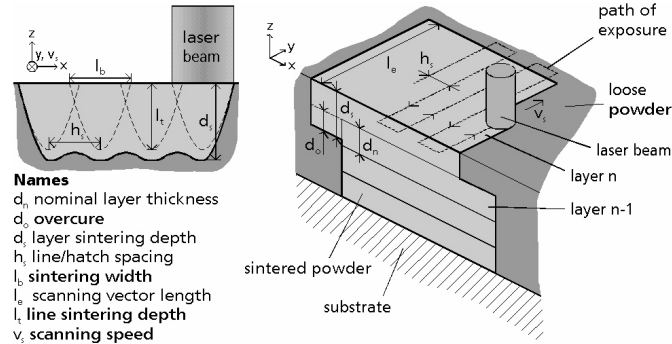


Fig. 2: Process parameters for SLS of borosilicate glass

A knowledge of the sinter depth  $d_s$  can serve to greatly reduce the number of investigations needed and approximating  $d_s$  for a given combination is a relatively fast process. Therefore, first the three main parameters were explored in single-layer trials:  $P_L$ ,  $v_s$  and  $h_s$  in order to determine the sinter depth and behavior. The single layers are  $20 \times 20 \text{ mm}^2$  and were exposed in a 2 mm deep powder bed. A target value of  $d_s = 0.2 \text{ mm}$  was chosen. Clearly  $d_s$  needs to be larger than the largest particle size and sufficiently large to provide sufficient adhesion to the previous layer. However it should also be kept relatively small in order to inhibit the thermal stresses resulting from the re-exposure of previous layers.

The initial results for borosilicate glass show the same trends as is known from ceramic SLS processes [3]. **Figure 3** shows a summary of the single layer investigations in terms for  $d_s$  versus  $P_L$ ,  $v_s$ , and  $h_s$ . An increase in  $P_L$  led to an increase in  $d_s$ , as shown in the top right graph for increasing  $P_L$  with  $h_s = 0.12 \text{ mm}$  and  $v_s = 500, 1000$  and  $2000 \text{ mm/s}$ . As anticipated,  $d_s$  also increases as  $v_s$  decreases, as shown in the bottom left graph for  $P_L = 14 \text{ W}$  and  $h_s = 0.03, 0.12, 0.21$  and  $0.3 \text{ mm}$ . As  $h_s$  is increased,  $d_s$  decreases within the range shown on the bottom right hand graph for  $P_L = 14 \text{ W}$  and  $v_s = 100, 200$  and  $300 \text{ mm/s}$ . From these results, parameter sets can be combined. For instance, for  $d_n = 100 \text{ }\mu\text{m}$ ,  $P_L = 14 \text{ W}$ ,  $h_s = 0.12 \text{ mm}$ , and  $d_s = 0.23 \text{ mm}$ , the optimal scan speed is approximately  $v_s = 400 \text{ mm/s}$ .

Cubes, a multilayer test geometry, were built in order to provide a more accurate analysis in terms of visual analysis, surface roughness and density. These cubes are  $20 \times 20 \times 10 \text{ mm}^3$ . This is a sufficient height for a visual analysis of side surface roughness and cracks. With these cubes, other parameters were then explored, such as  $d_n$  and the exposure strategy. The main parameters were varied from  $P_L = 5 - 94 \text{ W}$ ,  $v_s = 100 - 1300 \text{ mm/s}$  and  $h_s = 0.03 - 0.30 \text{ mm}$ . Parameter sets were matched from the single layer exposures for  $d_s \approx 0.2 \text{ mm}$ .  $d_n = 100 \text{ }\mu\text{m}$  and a layerwise alternating unidirectional exposure strategy was employed. The base plate used was of the same material composition to obtain better adhesion to the sintered part.

### Material

Borosilicate glass 3.3

### Machine Parameters

$P_L = 5 - 94 \text{ W}$

$v_s = 50 - 3000 \text{ mm/s}$

$h_s = 0.03 - 0.3 \text{ mm}$

### Geometry

$20 \times 20 \text{ mm}^2$ , single layer

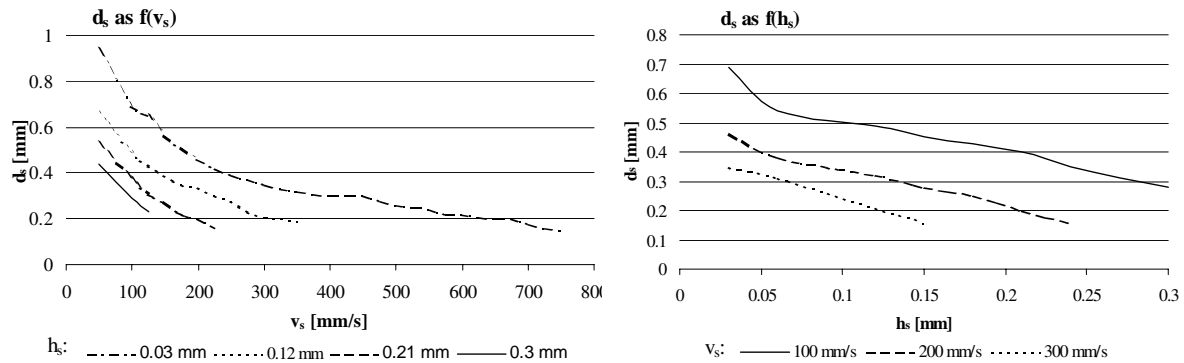


Fig. 3: Single layer experimental results – dependence of parameters on  $d_s$

Crack propagation was common for all parameter combinations. These crack profiles are visible over a number of layers, unlike with delamination. One theory for this is the thermal shock characteristics of borosilicate glass. Borosilicate glass, while more resilient than many glasses, is still known to have problems with accommodating rapid temperature changes of greater than  $5 \text{ }^\circ\text{C/min}$  [2]. The laser beam clearly introduces more heat in a shorter period of time, which may lead to thermal stresses within the sintered part and be a primary factor in the resultant crack profiles. Over 47 W, these cracks led to failure in the parts. Therefore the experiments were found to be only successful at low  $P_L$  and thereby low  $v_s$ . **Figure 4** shows the results for  $P_L = 14, 32$  and  $47 \text{ W}$  consecutively. It is visibly clear that at 14 W, the appearance of cracks is greatly reduced and the stability of the parts thereby improved. Hence  $P_L = 14 \text{ W}$  was taken as an upper limit for further investigations.

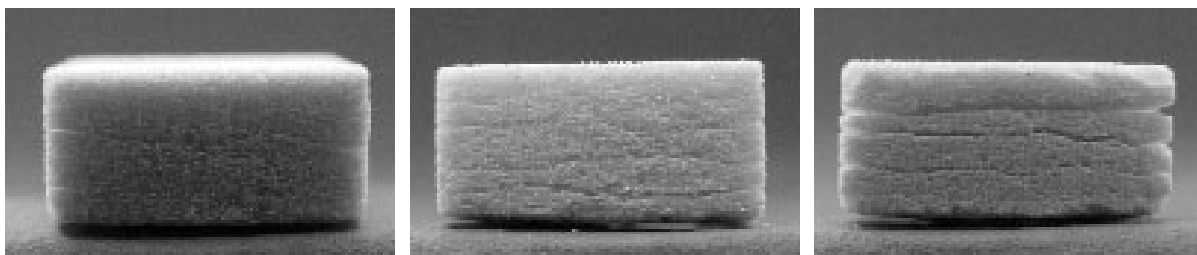


Fig. 4: Test geometry experimental results for increasing  $P_L$

Next  $h_s$  was varied over the range from 0.03 mm – 0.30 mm with a constant  $P_L = 9 \text{ W}$  and  $d_s \approx 0.2 \text{ mm}$ . While parts could be built over the entire range, the side surface appearance at  $h_s \leq 0.12 \text{ mm}$  was extremely poor. In **Figure 5** the differences are clearly visible: the left part was produced with  $h_s = 0.03$ , compared to the right part with  $h_s = 0.18 \text{ mm}$ , where the side surface is greatly improved. Furthermore, an upper limit on  $h_s$  was determined to be at

approximately 0.30 mm, because the top surface roughness was highly degraded above this value.

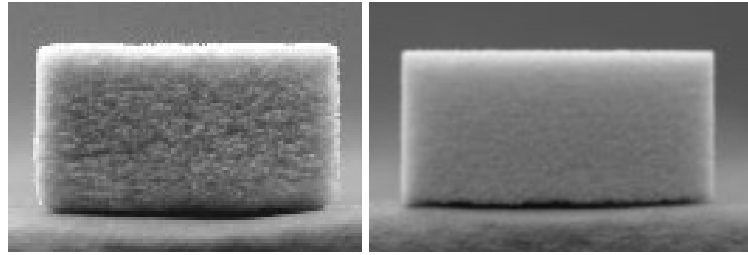


Fig. 5: Test geometry results for varied  $h_s$

Two main analysis parameters, the density and surface roughness  $R_z$ , were then considered for a range of parameters as shown in **Figure 6**. Again the same basic mechanisms were found to prevail. An increase in  $v_s$  leads to a decrease in the density of the specimen, shown in the top left graph. However,  $R_z$  also increases, as shown in the top right graph. Therefore choosing between higher density or lower  $R_z$  will still be a tradeoff when choosing an optimal  $v_s$ . The results for  $h_s$ , bottom left, show an increase in density at lower  $h_s$ . However the density seems to taper off at  $h_s = 0.18$  mm, and furthermore  $R_z$  shown on the bottom right, increases drastically above 0.18 mm, leading to the conclusion that there is no advantage to having  $h_s \geq 0.18$  mm. Furthermore, prior results indicated that the side surface was greatly degraded below  $h_s = 0.12$  mm, resulting in a narrow window of  $0.12 \leq h_s \leq 0.18$  mm.

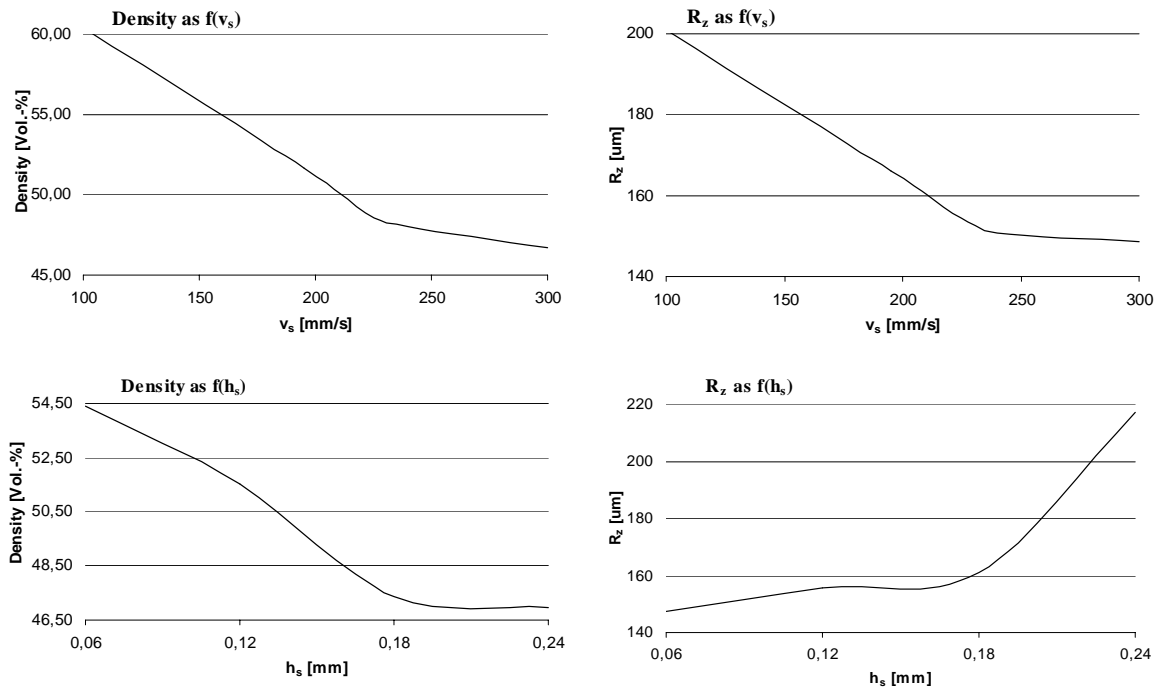


Fig. 6: Density and surface roughness  $R_z$  for increasing  $v_s$  (top) and  $h_s$  (bottom)

A secondary consideration was the dimensional accuracy of the parts. All of the parameter combinations which led to a successfully sintered part were slightly larger than the anticipated size (approx. 0.30 – 0.60 mm along each length). The most likely cause is the heat transferred by the laser beam. The sintered region differs from the region traversed by the center of the laser beam, resulting in slightly larger parts. Part growth is also caused by heat

transfer from the exposed part to the surrounding loose powder. These effects can however be compensated for with a beam compensation factor.

Investigations into the implementation of other exposure strategies, such as the stripes and chess exposure strategies, were also held. Both strategies benefit from shorter scan vector lengths, but often with a sacrifice in surface quality and part strength. For the employed geometry, a jump in density was seen with a 5 mm wide stripe or chess width. For the chess strategy, the resulting density, 49.5 %, was nearly a percent larger than with a unidirectional exposure strategy. However part strength was also greatly reduced as the parts were prone to break along the fill lines, or overlap, between chess squares. Furthermore the optimal stripe or chess size is largely dependent on the given part geometry.

Of all the parameter combinations that led to a stable laser sintering process, the maximum density achieved was 48.6 % of theoretical density ( $P_L = 9 \text{ W}$ ,  $v_s = 225 \text{ mm/s}$ ,  $h_s = 0.15 \text{ mm}$ ) with  $R_z = 152 \text{ }\mu\text{m}$ .

To examine the microstructure and better understand the density achieved, the sintered parts were then subject to a post-heat treatment in an oven for 6 hours at temperatures of 500 °C to 900 °C. As expected, there was no significant change in properties at 500 and 550 °C. At 600 °C, however, there is a small increase in the density (slightly less than 1 %), signaling that only at this point is the rearrangement of boron oxide, with a softening point of 450 °C, complete. At 700 °C, the part begins to shrink (3.1 %), but there is a significant increase in density from 49.7 % to 54.4 %. This trend continues at 750 °C where the part starts to deform and has shrunk an additional 5 %. At 800 °C, there is significant shrinkage (17 %) and warpage, but the part reaches nearly full-density and at 900 °C the part is no longer identifiable. This is consistent with the softening point of borosilicate glass at 820 °C. The SEM figures show correlating results. At 600 °C, there is much unsintered powder, however at 700 °C, more sintered structures are formed, and from 750 °C – 800 °C the pores close off to achieve near full density. These results are summarized in **Figure 7**.


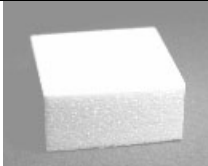
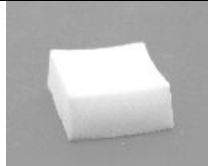
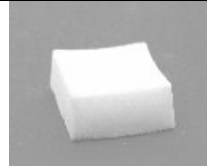



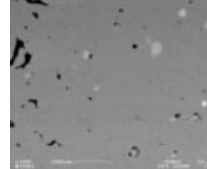
	600 °C	700 °C	750 °C	800 °C
<b>Test Geometry</b>				
<b>Microstructure</b>				
<b><math>\rho</math> (%)</b>	49.7	54.4	63.3	96.4
<b>Shrinkage (%)</b>	0	3.1	≈ 8.0	≈ 17.0

Fig. 7: Post-processing of laser sintered borosilicate glass

To determine if this density could be increased with the use of an additive, 0.05 % weight carbon black powder was mixed with the borosilicate glass powder. During the manufacturing of carbon black, aggregates are formed of primary particles which are only a few tens of nm in size. Due to the small size and the small distances between the aggregates, van der Waals forces are present, and as a result the aggregates cluster to form agglomerates. When mixed with borosilicate, the agglomerates break up to form a network of fine particles

with thousands of cubic meters of carbon black on the surface throughout the matrix. Thereby carbon black does not sinter but provides higher energy absorption sites allowing the borosilicate glass to more tightly absorb.

The addition of this powder increased the sinter depth of the mix, enabling the borosilicate glass to be sintered at slightly higher temperatures. There was however no significant increase in the viable parameter window. Comparing the results of a stable parameter set for both with and without carbon black, the carbon black led to a comparable surface roughness and a small increase in density of 0.8 %, **Figure 8**. Furthermore the use of carbon black necessitates the use of a post-processing step for removal.

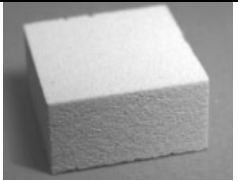
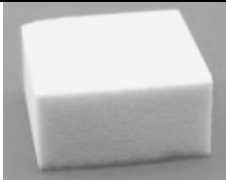
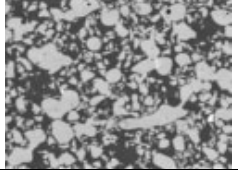
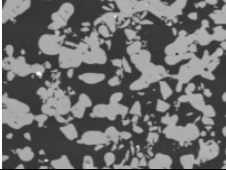
	<b>BSCG + 0.05 % Carbon Black</b>	<b>Only BSCG</b>
<b>Test Geometry</b>		
<b>Microstructure</b>		
<b>ρ (%)</b>	49.5	48.6

Fig. 8: Effect of carbon black additive on borosilicate glass SLS part

### Conclusion

Borosilicate parts could successfully be produced using SLS within the parameter window:  $P_L = 5 - 9$  W,  $v_s = 300 - 550$  mm/s and  $h_s = 0.12 - 0.18$  mm. One stable parameter combination was found to be:  $P_L = 9$  W,  $v_s = 225$  mm/s,  $h_s = 0.15$  mm and  $d_n = 0.10$  mm. This resulted in a density of 48.6 % of the theoretical density, an  $R_z$  of 152  $\mu$ m and a dimensional accuracy of 98 %. The major drawback was the appearance of crack profiles, which is assumed to be due to the thermal shock characteristics of borosilicate glass. One likely way to alleviate this problem is with the implementation of a heated powder bed in order to reduce the thermal gradients. A thermal post-processing at 700 °C results in a slightly denser part, 54.4 %, with a reduced appearance of cracks due to mechanism of viscous flow.

### References

- [1] Doremus, R.H. *Glass Science*. Wiley-Interscience (1994)
- [2] Robu Glasfilter-Geräte. *Sinterfilter Vitrapor: Technical Data*. <http://www.robuglas.com/>
- [3] Klocke, F., Wirtz, H. *Selective Laser Sintering of Zirconium Silicate*. Proceedings of the 9<sup>th</sup> Solid Freeform Fabrication Symposium, Austin, pp 605-612 (1998)